Essential Readings in Light Metals: Cast Shop for Aluminum Production.
Edited by John F. Grandfield and Dmitry G. Eskin.

Light Metals — From *Light Metals 1989*, Paul G. Campbell, Editor

MODELLLING OF FLUID FLOW AND STRESS PHENOMENA DURING DC CASTING OF ALUMINIUM ALLOYS

S.C.Flood*, L.Katgerman*, A.H.Langille+, S.Rogers* , C.M.Read+

Alcan International Limited

*Banbury Laboratories
Oxon, OX16 7SP
ENGLAND

+Kingston RDC
Ontario , K7L 5L9
CANADA

Alcan International Limited has established a research programme to investigate the fundamental physical processes which occur during DC casting.

As part of this effort, the solidification, heat and fluid flow and stress build-up during DC casting are being modelled mathematically in order to investigate the influence of the casting parameters, and thereby formulate recommendations for improvements in casting practice and mould design.

The thermal and fluid flow fields are calculated by the control volume finite difference technique using a modified version of the CFD package PHOENICS. The effect of natural convection in the liquid metal is included through the Boussinesq approximation.

The resulting thermal fields form the basis for a finite element calculation of the stress distribution arising from the thermal strains. The ANSYS package is used to calculate the stresses, assuming firstly elastic and then non-linear elastic behaviour, with temperature dependent material properties in both cases.

Results are presented to show the significance of the fluid flow prior to solidification and the nature of the stress distribution during casting. The differences between the linear and non-linear elastic calculations are illustrated.

INTRODUCTION

Alcan International Limited has established a research programme to investigate the fundamental physical processes which occur during DC casting in order to improve the metallurgist's ability to control the quality of the as-cast ingot. As part of this effort, numerical techniques are being used to simulate the thermal, fluid flow and stress fields which exist during casting and which determine the macro- and micro-structure, macrosegregation, porosity level and mechanical integrity of the product.

THE CALCULATIONS

Overview

The thermal and fluid flow fields are calculated by the control volume, finite difference technique, and the resulting thermal fields are then used as the basis for a finite element calculation of the stress distribution arising from thermal strains. The thermal calculations include the liberation of the latent heat of fusion. The k-ε model is used in the fluid region to provide for the increases in effective viscosity and thermal diffusivity due to turbulence. The stress calculations were originally purely elastic but now a non-linear elastic treatment is used in order to accommodate the temperature dependence of the mechanical properties and to allow an approximation for plastic yielding.

Formulation of the Thermal and Fluid Flow Calculations

Three dimensional rectangular cartesian and polar calculations have been performed. The steady-state conservation equations for enthalpy, mass and momentum are solved for temperature and the velocity components using a modified version of the CFD package PHOENICS (1). The SIMPLEST algorithm is used to couple the velocity and pressure fields such that the velocity field satisfies the continuity equation (2). A single phase formulation is adopted: the equation solved, in rectangular cartesian co-ordinates, for a variable ϕ is:

$$div.(\rho \underline{v}.\ \phi - \Gamma\, grad\, \phi) = S_\phi$$

- where S_ϕ is a source term per unit volume, ρ is density, $\underline{v}$ is velocity and Γ is an exchange coefficient.

The local proportion of solid, f_s ,is assumed to be a function of temperature: for complex alloys it is described by a function fitted to DSC measurements of latent heat evolution while, for binary alloys it is assumed to be given by the Scheil equation with a jump to $f_s = 1$ at the eutectic temperature:

$$f_s = \begin{cases} 0 & T > T_L \\ 1 - \left\{ \dfrac{T_p - T}{T_p - T_L} \right\}^{\frac{1}{k-1}} & T_L \geq T > T_E \\ 1 & T_E \geq T \end{cases}$$

(T_L = liquidus; T_E = eutectic temperature; T_p = melting point of pure metal; k = distribution coefficient). When solving for the temperature ($\phi = T$), Γ is λ/c (λ = thermal conductivity; c = specific heat capacity) and solidification is included in the source term:

$$S_T = \frac{\rho L}{c}\, div\,(\underline{v} f_s)$$

L is the specific latent heat of fusion. The large magnitude of L/c (300K for Al) necessitates relaxation to prevent destabilising fluctuations of the latent heat source. This relaxation is achieved by a technique based on the enthalpy-solid fraction relation together with additional, linear relaxation close to the liquidus temperature, where the solid fraction changes rapidly.

For velocities, the source term includes contributions arising from the pressure gradient in the liquid, the fixing of velocity in the solid and, in the case of the vertical component of velocity, a Boussinesq buoyancy source term.

The interaction of the solidifying mush with the velocity field in the liquid is complicated but is approximated by forcing the local velocity towards the casting speed by source terms dependent on the local solid fraction. The form of the functional dependency on solid fraction of these source terms is debatable. Two possibilities that have been explored are:

(i) to use the Kozeny-Carman equation to gradually decrease the permeability as a function of increasing solid fraction (3) and,

(ii) to fix the local velocity to the casting speed when $f_s \geq 0.1$ (4).

The fixing of the velocity is achieved by d'Arcy sources of the form:

$$S_\phi = C(V_{fix} - \phi)$$

- where C is related to the reciprocal of the permeability and V_{fix} is the relevant component of the casting velocity.

The Boussinesq buoyancy source term appears in the equation for the velocity component in the direction of gravity, and is of the form:

$$S = \rho_{ref}\, g\, \beta\, (T - T_{ref})$$

where

$$\beta = \frac{1}{\rho_{ref}} \cdot \frac{d\rho}{dT} \quad (approx. -10^{-4} K^{-1} \text{ for Al})$$

The k-ε model (5) is used to introduce turbulence, and when this is used, the velocities that are solved for are the time-averaged values. There are many methods (6,7,8) for treating turbulent flow and each would seem to have certain advantages and although more complicated models are being developed, the k-ε model is still used frequently for solving engineering problems. The mean component of turbulence is solved for in terms of the turbulent kinetic energy, k, and the dissipation rate, ε, and these two quantities give an indication of the size of the fluctuating component ($k^{\frac{1}{2}}$), the turbulent viscosity (k^2/ε)and the length scale of the turbulence ($k^{3/2}/\varepsilon$). The turbulent viscosity is used to boost the laminar value, thus simulating the effect of the Reynolds stresses. Similarly, the thermal diffusivity is also boosted in relation to the turbulent viscosity to reflect enhanced thermal transport due to turbulent mixing.

Thermal Stress Calculations

The thermal stresses arising from the temperature distribution in the ingot are calculated using the ANSYS package (9), which employs standard finite element techniques (10,11).

The solidified metal is either treated as an isotropic linear elastic medium with a temperature dependent modulus given by 80–0.044T GPa (T in Kelvin) (12) or as a non-linear elastic medium to simulate yielding at different temperatures *(Figure 1)*.

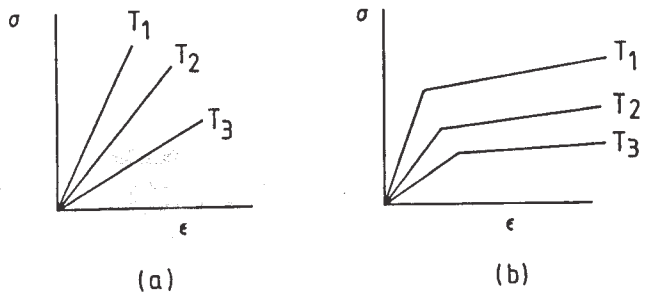

Figure 1
Temperature dependent (a) elastic and (b) non-linear elastic material behaviour

COMPARISON OF MEASURED AND CALCULATED SUMP SHAPES

Excellent agreement has been obtained between the shape of the solidification front determined by decoration by copper addition during casting and that determined numerically *(see Figure 2)*, and this was seen to support the validity of the model. Good agreement has also been obtained between measured and calculated temperature traces for thermocouples inserted into an ingot during casting.

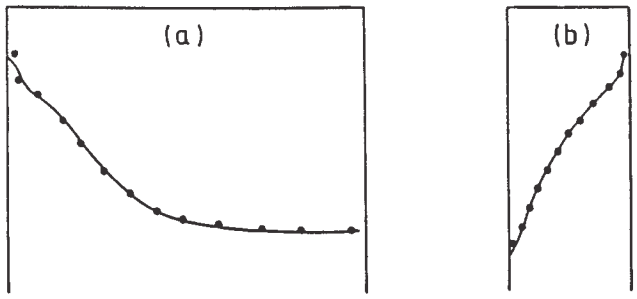

Figure 2
Comparison of measured (dots) and calculated (line) solidification fronts along the planes of symmetry of a DC ingot. (a) Parallel and (b) perpendicular to the rolling face.

DISCUSSION

Thermal and Fluid Flow Calculations

It is apparent that there is a competition between the thermally driven buoyancy and the inlet velocity. The former dominates unless the inlet velocity is high. The fluid flow results are illustrated with reference to the axi-symmetric case, i.e. a cylindrical ingot. In *Figure 3(a)*, when the inflow is over the entire top surface, the buoyancy forces determine the flow, but in *Figure 3(b)*, when the flow is restricted to one tenth of the top surface and the inlet velocity is one hundred times greater, then the inlet velocity dominates and the direction of rotation of the flow is reversed. When buoyancy is influential it produces flat isotherms throughout most of the liquid and steep temperature gradients close to the mush, and the flow is predominantly down the front of the mush with a slow recirculation elsewhere. With a high inlet velocity, the buoyancy can be overridden and penetration of the sump can produce both a different shape of mushy zone and a very different flow pattern.

The description of the permeability of the mush affects the stability of the calculations and the calculated shape of the mush. *Figure 4(a)* shows the effect of using the Kozeny-Carman equation instead of, as in *Figure 3(b)*,simply imposing a severe d'Arcy source for $f_s \geq 0.1$.

The two diagrams in *Figure 4* show the effect of turbulence. Turbulence enhances thermal diffusion producing less cramped isotherms and a smoother liquidus shape but the solidification pattern is not affected after $f_s = 0.1$.

Thermal Stress Calculations

In a previous series of calculations it was demonstrated that the rate of heat extraction affects stress levels more than the casting speed [4].

The different stress levels calculated using the linear and non-linear elastic treatments are shown in Figures 5 and 6. In the non-linear elastic case , the material is allowed to "yield" and consequently, the level of stress is substantially lower than in the elastic calculations. The stress distibutions are also quite different : the non-linear elastic results indicate that the equivalent stress at the centre of the rolling face and corner of the ingot are similar whereas the elastic results suggest that that at the centre of the rolling face should be much higher than that at the corner.

a) Inflow Over Entire Top Surface

b) Inflow Restricted to 10% of Radius

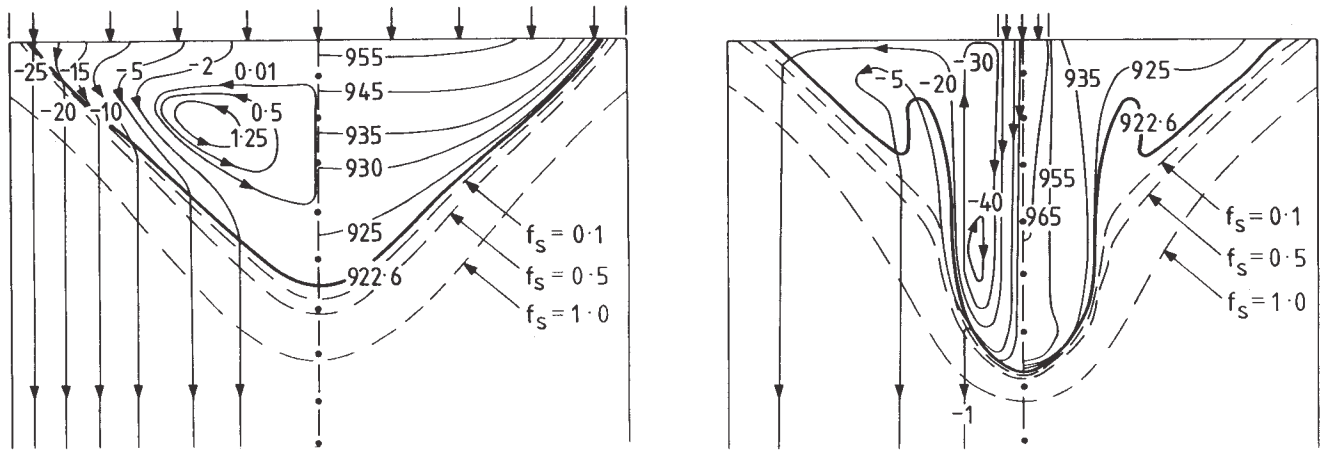

Figure 3
Cylindrical ingot (550mm diameter) of Al-4 wt%Cu, cast at 45mm/min and 968K. D'Arcy source imposed abruptly for fs ≥ 0.1. Laminar calculation-enhanced kinematic viscosity. Streamlines on left ; isotherms on right (in K)

a) Inflow Restricted to 10% of Radius (Laminar)

b) Inflow Restricted to 10% of Radius (Turbulent)

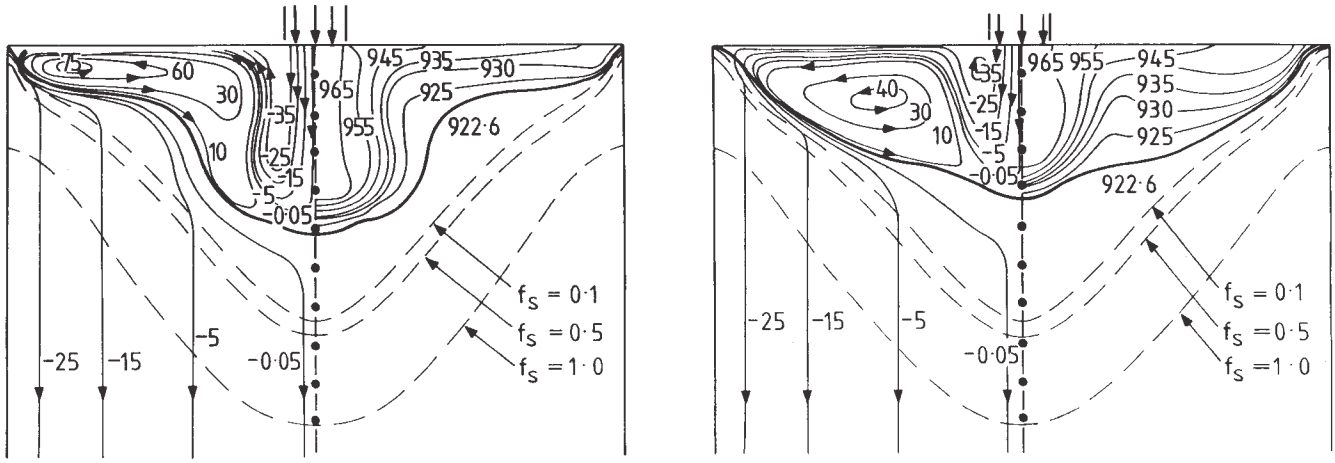

Figure 4
Cylindrical ingot (550mm diameter) of Al-4 wt% Cu, cast at 50mm/min and 968K. (Kozeny-Carman equation used) Vertical inflow , restricted to 10% of radius.
(a) Laminar calculation - enhanced kinematic viscosity (5.5×10^{-5} $m^2 s^{-1}$).
(b) Turbulent Calculation (k - ε model)
Streamlines on left ; isotherms on right (in K)

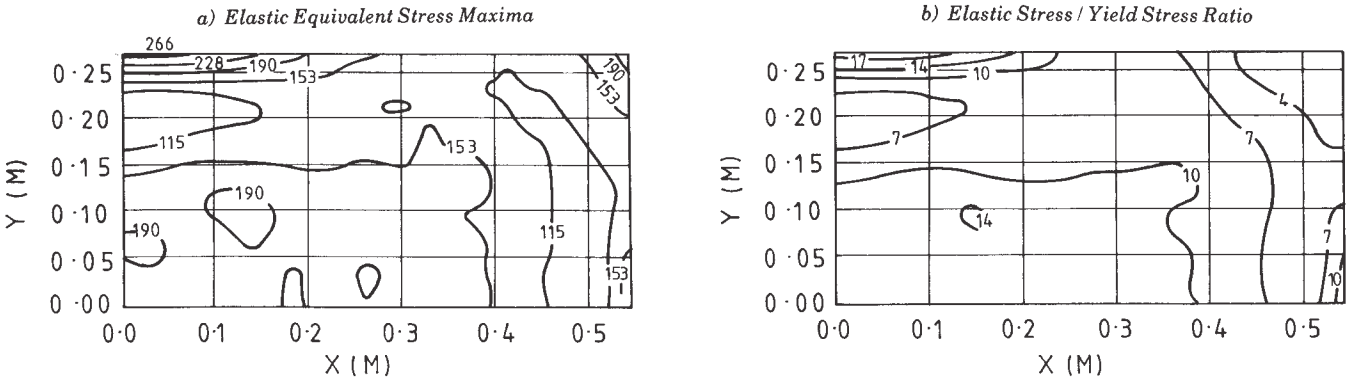

Figure 5
Elastic Stress Distrubution
(a) Equivalent stress and (b) equivalent stress normalised with respect to the temperature dependant yield stress for a horizontal cross-section of a rectangular ingot.
Only a quarter of the ingot is shown, centre at (0,0)

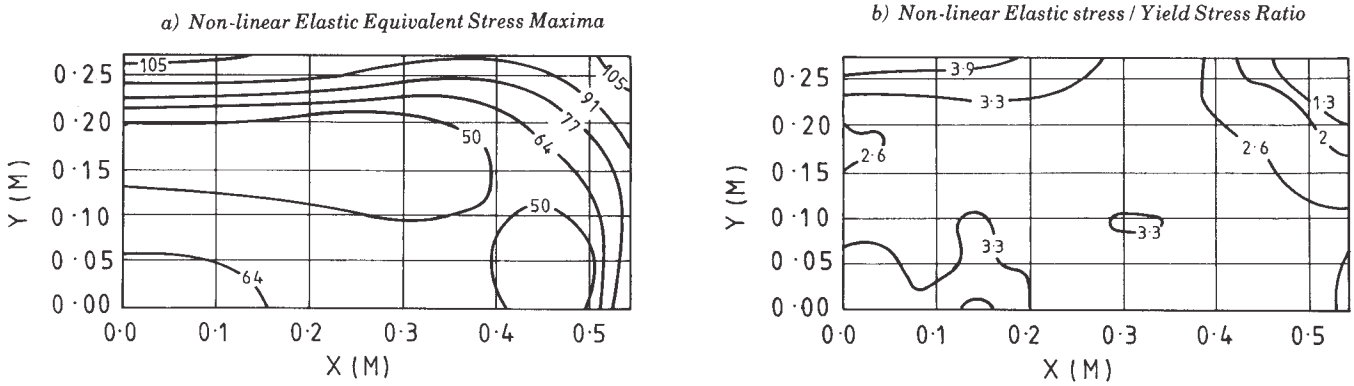

Figure 6
Non-linear stress distribution
(for details see Figure 5 captions)

In order to predict the susceptibility of the ingot to cracking, it is necessary to interpret the calculated stresses in the light of the temperature trends of the mechanical behaviour of the alloy. Therefore, cracking susceptibility is discussed in terms of a dimensionless group (the stress ratio) formed by dividing the calculated equivalent stress by the yield stress as a function of temperature. Consider Figures 5 and 6. The stress and stress ratio distributions differ substantially : the latter show high ratios at the centre of the ingot and thereby indicate a greater relative susceptibility to cracking there than is anticipated from the equivalent stress distributions. The non-elastic ratios are far smaller than the elastic ones and therefore suggest a lower susceptibility to cracking than do the elastic calculations, reflecting the difference in the stress levels produced in the linear and non-linear elastic treatments.

From the differences in level and distribution it is clear that a non-linear elastic approach is required in order best to predict cold cracking during DC casting.

CONCLUSIONS

Fluid Flow

1. Sump shape is influenced significantly by the entry conditions only when the entry velocity is high.

2. Buoyancy dominates the flow pattern when the entry velocity is low.

3. Turbulence enhances thermal diffusion and produces a smoother solidification front.

Thermal Stress

1. Non-linear elastic stress calculations are required to predict the occurrence of cold cracks.

ACKNOWLEDGEMENTS

The authors would like to thank Dr. J.D. Clark for valuable discussions in the course of this work and Messrs. J. Worth and K. Kasai for practical help.

REFERENCES

1. PHOENICS. CHAM Limited, London, SW19 5AU, England.

2. D.B. Spalding. Mathematical Modelling of Fluid Mechanics, Heat Transfer, and Chemical Reaction Processes. A Lecture Course. CFDU Report HTS/80/1, Imperial College, London.

3. V. Voller and C. Prakash, *"A Fixed Grid Numerical Modelling Methodology for Convection-Diffusion Mushy Region Phase Change Problems"*, Int. J. Ht. Mass Tfr, 30 (1987) p.1709-1719.

4. S.C. Flood, L. Katgerman, A.H. Langille and C.M. Read, *"A Model of Solidification, Fluid Flow and Stress Distribution in D.C. Casting"*, presented at Modeling of Casting and Welding Processes IV, Palm Coast, Florida (April 1988), in press.

5. B.E. Launder and D.B. Spalding, *"The Numerical Computation of Turbulent Flows"*, Comp-Meth Appl. Mech. Eng., 3 (1974), 269- 289.

6. J.L. Lumley. Prediction Methods for Turbulent Flows. VKI Lecture Series, 76, (1975).

7. A. Leonard, *"Review of Vortex Dynamics for Flow Simulation"*, J. Comp. Phys., 37, (1980), 289.

8. P. Bradshaw. Topics in Applied Physics: Turbulence. Springer Verlag, Heidelberg.

9. ANSYS. Swanson Analysis Systems Inc., Pennsylvania 15342, USA.

10. ANSYS. Theoretical Manual (Swanson Analysis Systems Inc., 1986).

11. O.C. Zienkiewicz. The Finite Element Method (3rd Ed., McGraw- Hill, London, (1977).

12. L.E. Mondolfo. Aluminium Alloys Structure and Properties (Butterworths, London, 1976).